LWT - Food Science and Technology 63 (2015) 1206–1213

Contents lists available at ScienceDirect

LWT - Food Science and Technology

journal homepage: www.elsevier.com/locate/lwt

Development of silver/titanium dioxide/chitosan adipate nanocomposite as an antibacterial coating for fruit storage

Baofeng Lin [a, b], Yaguang Luo [b, *], Zi Teng [c], Boce Zhang [b, c], Bin Zhou [b, c], Qin Wang [c]

[a] College of Chemistry and Chemical Engineering, Guangxi University, Nanning 530004, China
[b] Food Quality Laboratory, Agricultural Research Service, the United States Department of Agriculture, Beltsville, MD 20705, United States
[c] Department of Nutrition and Food Science, University of Maryland, 0112 Skinner Building, College Park, MD 20742, United States

ARTICLE INFO

Article history:
Received 23 October 2014
Received in revised form
16 April 2015
Accepted 19 April 2015
Available online 25 April 2015

Keywords:
Silver
Titanium dioxide
Chitosan adipate
Nanocomposite
Antibacterial coating

ABSTRACT

A novel nanocomposite of silver/titanium dioxide/chitosan adipate ($Ag/TiO_2/CS$) was developed through photochemical reduction using a chitosan adipate template. Chitosan served as a reducing agent anchoring the metal ions through Ag—N coordination bonds and electrostatic attractions, thus stabilizing the $Ag/TiO_2/CS$ product observed by Fourier transform infrared spectroscopy and X-ray diffraction patterns. Scanning electron microscopy observations revealed that the nanocomposite particles (50–100 nm) were deposited onto the chitosan adipate layer. The product exhibited high ζ-potentials from 30.1 mV to 33.0 mV during 60 days of storage. In addition, the nanocomposite demonstrated higher antimicrobial activity than $AgNO_3$ or nano-Ag particles at similar concentrations, as evidenced by the inhibition zone, minimum inhibitory concentrations (MIC), and growth curve. The nanocomposite reduced the *Escherichia coli* population by 6 logs after 24 h of incubation, and had an MIC value of 0.38 μg Ag/mL. These results suggest that $Ag/TiO_2/CS$ has the potential to be used as an antibacterial protective coating for fruit storage.

1. Introduction

Chitosan is a biodegradable polysaccharide composed of N-acetyl-D-glucosamine and D-glucosamine, generated by the alkaline deacetylation of chitin (Onishi & Machida, 1999). It is the second most abundant natural biopolymer and relatively inexpensive (Ma et al., 2008). In addition, it is recognized as a nontoxic, biodegradable, biocompatible and environmentally-friendly material. Many properties that are beneficial for a protective fruit coating, including film forming capability and antibacterial effects (Vásconez, Flores, Campos, Alvarado, & Gerschenson, 2009). Nevertheless, chitosan has a few drawbacks, such as pH-dependent solubility, which can be overcome by using chitosan salts (Belalia, Grelier, Benaissa, & Coma, 2008), and high viscosity, which makes the coating slow to dry and difficult to attach in some gaps on the surface of fruits (Lin et al., 2011) thus impeding its antibacterial ability. In addition, fruits produce moisture and gaseous metabolites continuously during storage due to respiration. Respiration rates depend on storage temperature, time since harvest, commodity and condition (damaged vs intact). Chitosan coatings on the surface of fruits may initially be wet and sticky, which could discourage sales of coated fruits. Furthermore, despite initial wetness, chitosan coatings become dry and develop cracks over time. Therefore, chitosan or chitosan-based coatings have only limited short-term antibacterial effect (Geisberger et al., 2013).

Silver nanoparticles are of particular interest due to their unique properties, like the broad-spectrum of bactericidal activities, which can be incorporated for long-term antibacterial performance as non-edible coatings or additives in food packaging (Reidy, Haase, Luch, Dawson, & Lynch, 2013). Although excessive oral consumption of silver may cause acute immunological response or chronic argyria, the amount of silver that could migrate from the composite to the fruit surface and thus be ingested should be well below the lowest reported effect level of 0.5 mg/kg of bw/day in animal studies (Park et al., 2014) and well below levels typically found to cause toxic effects in humans (Hadrup & Lam, 2014). Silver and silver colloids have numerous applications in various fields because of their broad spectrum antimicrobial activity. The toxicity of silver nanoparticles depends on particle size. Particles sizing 15 nm and 30 nm have higher toxicity than those sizing 55 nm particles, and they were shown to have a slight cytotoxic effect on eukaryotic cells at concentrations greater than or equal to 75 μg/mL (Carlson et al., 2008).

* Corresponding author. Tel.: +1 3015046186; fax: +1 3015045107.
E-mail address: Yaguang.Luo@ars.usda.gov (Y. Luo).

http://dx.doi.org/10.1016/j.lwt.2015.04.049
0023-6438/

In this study, the 50–100 nm nanoparticles were effective at inhibiting *Escherichia coli* cells at an MIC of 0.38 μg/mL, thus allowing a safe concentration despite potential particle migration. Many techniques have been investigated for the production of silver nanoparticles, including chemical reduction, electrochemical reduction, photochemical reduction, gamma-ray irradiation, UV irradiation, ultrasonic method, and microwave method (Byeon & Kim, 2012; Hettiarachchi & Wickramarachchi, 2011; Nadagouda, Speth, & Varma, 2011; Spadaro, Barletta, Barreca, Curro, & Neri, 2010). Various stabilizers have been used in these processes to achieve the desirable particle size, size distribution, shape, stability, and solubility of silver nanoparticles. The most commonly used stabilizers are synthetic polymers such as polyvinyl pyrrolidone (PVP), polyvinyl alcohol (PVA), polyaniline, and polyethylene glycol (PEG) (Bouazza, Alonzo, & Hauchard, 2009; Tan, Dai, Li, & Zhu, 2003). Additionally, natural polymers such as starch (Hu, Wang, Wang, Zhang, & Yu, 2008) and chitosan (Hettiarachchi & Wickramarachchi, 2011) have been studied as potential stabilizers because of their biocompatibility and biodegradability. Incorporation of metal ions into chitosan tripolyphosphate nanoparticles was found to enhance antimicrobial activity (Du, Niu, Xu, Xu, & Fan, 2009).

Titanium dioxide (TiO_2), a metal oxide semiconductor, is a promising photocatalyst due to its desirable catalytic efficiency, chemical stability, low toxicity, and acceptable cost (Egerton & Tooley, 2004; Tong, Binh, Kelly, Gaillard, & Gray, 2013). Nano-TiO_2 exhibits good adhesiveness and bactericidal activities and has been used as a generally recognized as safe (GRAS) additive in medical devices and biomaterials (Kochkodan, Tsarenko, Potapchenko, Kosinova, & Goncharuk, 2008). However, the commercial applications of nano-TiO_2 are limited due to its unstable thermodynamic properties and tendency to agglomerate. The photocatalytic activity of nano-TiO_2 is activated by UV light in the presence of oxygen and water molecules, and it results in the production of reactive oxygen species and hydroxyl radical that are responsible for the bactericidal function (Banerjee, Gopal, Muraleedharan, Tyagi, & Raj, 2006). Thus UV light exposure is necessary for nano-TiO_2 to exert strong antibacterial activity, beyond that achieved with either UV exposure alone or nano-TiO_2 alone (Banerjee et al., 2006). Titanium dioxide coating on substrates is considered to be a contact-active antibacterial agent because it kills bacteria in close proximity efficiently without releasing biocides, and its antibacterial performance is restricted to the coated surface (Yuan, Ji, Fu, & Shen, 2008).

The objective of this study is to construct an antibacterial coating of Ag/TiO_2/CS for the storage of fruits with rough skin, such as cantaloupes and lychees, to reduce bacterial proliferation in the cracks and pores. In order to enhance the water solubility of chitosan, we used adipic acid to produce chitosan salts. Such products are suitable for use in fruit coating because they do not cause tissue damage. The TiO_2 nanoparticles were incorporated into the chitosan adipate solution and silver ions supplied by $AgNO_3$ solution were then loaded onto the formed template and reduced in-situ, forming silver deposited TiO_2 nanocomposite particles. The nanocomposite Ag/TiO_2/CS product was characterized in terms of ζ-potential, particle size, surface charge, FTIR spectrophotometry, X-ray diffraction patterns, and scanning electron microscopy (SEM). The antimicrobial activity of Ag/TiO_2/CS was tested against non-toxigenic *E. coli* O157:H7.

2. Materials and methods

2.1. Materials and reagents

Chitosan with 77% deacetylation and medium molecular weight and TiO_2 nanoparticles with average diameter of 21 nm were purchased from Sigma–Aldrich (St. Louis, MO, USA). All other reagents were of analytical grade.

2.2. Sample preparation

The first step in preparing the Ag/TiO_2/CS was the modification of chitosan to form its adipate salt (Lin, Wang, Li, Liang, & Du, 2012). A mixture of chitosan and adipic acid (-NH_2:-COOH = 1:1.2, molar ratio) was ground in a mortar using a pestle under semidry condition at room temperature until the mixture was water-soluble. The chitosan adipate product was washed using ethanol, dried at 50 °C for 2 h, and ground into powder.

A chitosan adipate aqueous solution (10 mg/mL, 2 mL) was prepared and mixed with $AgNO_3$ solution (10 mg/mL, 5 mL). The mixture was stirred magnetically for approximately 1 h in a water bath at 50 °C. Meanwhile, 0.10 g of TiO_2 particles were dispersed in 20 mL of distilled water in an ultrasound bath for approximately 10 min. Subsequently, a 200 μL aliquot of the TiO_2 dispersion was added into the Ag/chitosan adipate solution, which was then incubated at 50 °C for 0.5 h in the water bath. The solution was treated with UV radiation (15 W/m^2 = 365 nm) for 10 min to produce the Ag/TiO_2/CS nanocomposite. The Ag/CS and TiO_2/CS control samples were prepared under the same conditions as Ag/TiO_2/CS nanocomposite except that the Ag/CS and TiO_2/CS samples did not contain TiO_2 and $AgNO_3$, respectively.

Fig. 1 shows the schematic for the preparation of Ag/TiO_2/CS by UV irradiation (Lu et al., 2011). The conduction band of TiO_2 is represented by CB and VB. Under ultraviolet exposure, the silver ion (Ag^+) in $AgNO_3$ is reduced to elemental silver (Ag) in the presence of TiO_2 nanoparticles as a catalyst. Ultraviolet radiation facilitates electron transfer from TiO_2 to Ag^+ where it is stored temporarily in the conduction band of TiO_2 for Ag^+ reduction. The resulting Ag is deposited on the surface of the TiO_2 nanoparticles; meanwhile, it forms a complex with chitosan via Ag–NH_3 coordination bonds through the amino groups on chitosan.

2.3. Determination of ζ-potential and particle sizes of nanocomposite

The particle size was determined by dynamic laser scattering (DLS) using a BI-200 SM Goniometer Version 2 (Brookhaven Instrument Corp., Holtsville, NY). Particle dispersions in deionized water were measured without dilution. The refractive index and viscosity of water were applied to obtain accurate results. The laser power and aperture size were set consistently at 10 mW and

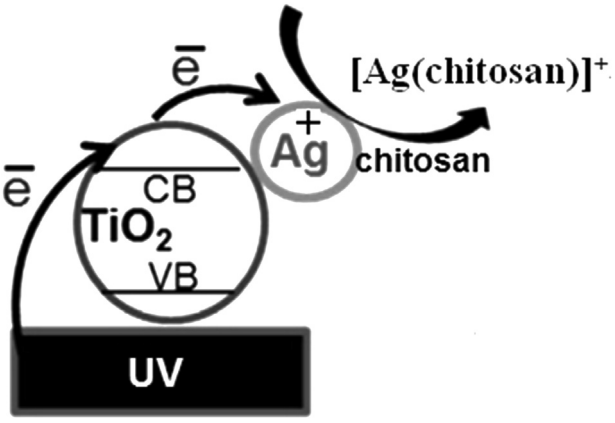

Fig. 1. Schematic view of the effects of UV irradiation on the formation of Ag/TiO_2/CS nanoparticles. CB and VB refer to conduction and valance bands respectively.

400 μm, respectively. All of the analyses were conducted at 25 °C for 1 min. Electrophoretic mobility of nanoparticle dispersions in deionized water was determined by laser Doppler velocimetry using a Nano ZS90 Zetasizer (Malvern, U.K.). Each sample was measured three times, and at least 12 runs were performed per measurement. The data was then automatically converted to ζ-potentials using the Smoluchowski model, which was carried by the supplier's software.

2.4. Infrared analysis

A Jasco 4100 series Fourier Transform Infrared Spectroscopy (FTIR) spectrometer with an attenuated total reflection (ATR) cell (Jasco Inc., Easton, MD) was used to monitor the structural changes of different samples. The samples were cast-dried on an aluminum tray for 24 h before mounting directly on the ATR cell. Spectra were acquired at 400–4000 cm^{-1} wavenumbers with a resolution of 4 cm^{-1}. The spectra were averaged and smoothed by adaptive smoothing using a convolution width of 5, and their baselines were calibrated with the Spectra Manager software (Jasco Inc., Easton, MD, USA). The resulting spectra were further analyzed by OMNIC software (version 8.0, Thermo Nicolet Corporation, USA).

2.5. Morphology and elemental analysis

The morphology and elemental composition were analyzed using scanning electron microscopy with energy dispersive spectroscopy (SEM/EDS) using a Hitachi SU-70 microscope (Pleasanton, CA, USA). Before measurement, the nanocomposite samples were cast-dried on an aluminum tray, mounted on a conductive carbon tape, and coated with gold/platinum. Both typical SEM and EDS digital images of the samples were reported.

2.6. X-ray diffraction (XRD) analysis

The XRD patterns of $AgNO_3$, TiO_2, chitosan and nanocomposite of Ag/TiO_2/CS were recorded on a Bruker D8-Advance Diffractometer (Bruker AXS Inc., Madison, WI, USA) using sample holders without backgrounds. The working parameters were voltage of 40 kV, current of 40 mA, and scanning rate of 3 min^{-1}.

2.7. Inhibition zone

Cultures for experiments (*E. coli* O157:H7: ATCC 700728, nontoxigenic) were prepared in Trypticase soy broth (TSB), incubated with agitation at 37 °C for 24 h, and then diluted 100 times with phosphate-buffered saline (PBS) to obtain the population of 10^6 CFU/mL. The Tryptic Soy Agar (TSA) medium was prepared, inoculated with *E. coli*, and dried in a biosafety hood for 30 min. Sterile absorbent paper disks (diameter 6 mm) were soaked overnight in treatment solutions containing Ag/TO_2/CS, chitosan, nanosilver, $AgNO_3$, TiO_2, or CS/Ag. The disks were dried in the biohood, placed at the center of the inoculated TSA, and incubated overnight at 37 °C. The experiment was performed in triplicate. The diameter of the inhibition zone around each disk was measured as an indicator of antibacterial activity (Guzmán, Dille, & Godet, 2009).

2.8. The minimum inhibitory concentration (MIC)

The MIC of each of the six sample treatments against *E. coli* O157:H7 was determined using the modified broth dilution method (Ollar et al., 1991). The samples were diluted using TSB, pH 7.0 to give final concentrations of 0, 10, 100, and 1000 μg/mL and inoculated with 100 μL of *E. coli* 157:H7 inoculum at a final concentration of 10^5 CFU/mL. Tubes were then incubated with shaking at 35 °C for 24 h and measured for their turbidity at 550 nm according to a previously reported method (Holowachuk, Bal'a, & Buddington, 2003). The MIC was defined as the lowest concentration at which no growth was observed, indicated by an absence of turbidity and/or unchanged absorbance.

2.9. Spectrophotometric analysis of E. coli O157:H7 growth inhibition

The effect of novel complexes on the growth of *E. coli* O157:H7 was also determined using a PerkinElmer Victor X3 multilabel plate reader (PerkinElmer, Inc., Waltham, MA). Spectrophotometric growth curves were obtained for the *E. coli* cultures in a 96-well microplate containing Ag/TiO_2/CS nanocomposite (both freshly prepared and stored for 60 days), $AgNO_3$, TiO_2, nanosilver, and control culture in TSB at pH 7.0 with no antimicrobials. All compounds were tested at a concentration of 100 μg/mL. The optical density of each well was automatically measured at 550 nm (OD550) every 10 min for 24 h, with shaking for 5 s before each measurement and incubation at 37 °C. Statistically significant difference between two conditions was established by performing Student's t-test (two sided) and was indicated by a P value less than 0.05. Each sample was tested in triplicate (Holowachuk et al., 2003).

2.10. Contact angle measurement

The contact angles of the nanocomposite dispersion and water were tested on cantaloupe rind by the sessile drop method using an Attension Theta tensiometer (Biolin Scientific, Linthicum Heights, MD, USA). Fresh cantaloupes purchased from a local grocer in College Park, MD, USA, were stored at 4 °C, and tested within 1 day. The droplet volume was 50 μL, and the advancing and receding droplets of water were controlled by an automated liquid dispenser (C201, Biolin Scientific). The data recording (60 fps) was triggered by the initial contact between the liquid droplet and the rind surface. All measurements were carried out under ambient conditions.

3. Results and discussion

3.1. Surface charge and particle sizes of nanocomposite

The ζ-potential of a dispersion represents the potential difference between the dispersion medium and the stationary layer of fluid attached to the dispersed particle. It is an important indicator of the stability of colloidal dispersions. The value of the ζ-potential denotes the degree of electrostatic repulsion between adjacent, similarly charged particles in a dispersion. For molecules and particles, a high ζ-potential confers stability, indicating that the solution or dispersion will resist aggregation/flocculation. According to the American Society for Testing and Materials,ζ-potentials with an absolute value higher than 30 mV are indicative of “moderate to good” stability of colloidal systems, owing to the strong electrostatic repulsion between the charged particles (Teng, Luo, & Wang, 2012).

The ζ-potentials of nano-Ag, nano-TiO_2, and chitosan adipate dispersion (in an acidic medium) were −29.5 ± 0.8, −15.6 ± 1.0, and 52 ± 1.65 mV, respectively. The ζ-potential of freshly prepared Ag/TiO_2/CS nanocomposite was 30.1 ± 0.9 mV, and it increased slightly to 33.9 ± 1.4 mV after 60 days of storage at 25 °C. These results evidenced successful coating of chitosan on the surface of nanocomposite particles and suggested that the samples were stable during the storage period. The interaction among CS, silver ions, and nano-TiO_2 in water solution was possibly promoted by the electrostatic force as CS carried positive charges, whereas nano-Ag and nano-TiO_2 were negatively charged. Furthermore, upon the addition of adipic acid at pH of 5–6, the amine groups of chitosan

were protonated to ammonium (Lin et al., 2011; Lin et al., 2012), thus adding to the positive charges of CS. This phenomenon facilitated the formation and also prevented the aggregation of Ag/TiO_2/CS nanocomposite.

Fig. 2A and B represent the size distributions of Ag/TiO_2/CS nanocomposite particles that were freshly prepared and stored for 60 days, respectively. A group of particles (50–100 nm) was observed in both diagrams. The particle sizes were not normally distributed, which is partially an artifact of the size of the silver nanoparticles purchased from Sigma Aldrich which were 50–100 nm and partially due to the selection of the smaller particles within that range for use in the coating and the presence of a trivial amount of larger particles formed via aggregation or coacervation. However, all particles were less than 100 nm, which further confirmed the stability of Ag/TiO_2/CS nanocomposite particles during storage, indicating that chitosan is a suitable stabilizer for the preparation of metal nanoparticles.

3.2. FTIR study

The FTIR spectra of chitosan (A) and Ag/TiO_2/CS nanocomposite (B) are presented in Fig. 3. When the physicochemical environment in the proximity of a functional group is changed (e.g., complexation between a ligand and a metal ion), its characteristic peak changes accordingly in its position and/or intensity. Chitosan exhibited two major peaks at 1642 (C=O stretching) and 1518 (N–H bending) cm^{-1}, respectively (Fig. 3A). These results were consistent with previous studies on chitosan (Luo, Zhang, Cheng, & Wang, 2011). In the nanocomposite FTIR spectrum, these two peaks shifted respectively to 1692 cm^{-1} and 1516 cm^{-1}, indicating the attachment of silver to the amide on chitosan. Moreover, a new band with high intensity was observed at 1314 cm^{-1} in the nanocomposite, possibly attributable to the newly formed Ag^{+}-N coordination bonds, because the peak did not appear on the chitosan spectrum (Zhang, Luo, & Wang, 2010). Chitosan has strong affinity towards metal ions because of the presence of numerous amine and hydroxyl groups (Wei, Sun, Qian, Ye, & Ma, 2009).

3.3. Morphology and elemental analysis

The morphology of the nanocomposite can be observed in the scanning electron micrographs shown in Fig. 4. A clear view of tree-like fractal structure was observed for CS (Fig. 4A), which was consistent with previous reports (Murugadoss & Chattopadhyay, 2008). (Fig. 4B), Irregularly shaped aggregates of silver/titanium dioxide were found on the chitosan adipate template of the nanocomposite sample. At higher magnification (Fig. 4C and D), these aggregates were observed to contain 50–100 nm particles, which were confirmed as silver and nano-TiO_2 particles by EDS (Fig. 4E and F). The spheroid or oblate spheroid particles (Fig. 4C) tended to form microsized aggregates (Fig. 4B). The EDS image (Fig. 4E), shows a nonuniform distribution of silver (green) on the surface of TiO_2 (red). Table 1 displayed the elemental composition of a single particle marked with a green cross in Fig. 4D. The results indicated that titanium, silver and carbon were the constitutive elements of the nanoparticles prepared by this photochemical reduction method, verifying the formation of Ag/TiO_2/CS nanocomposite.

3.4. XRD analysis of nanocomposite

The formation of Ag/TiO_2/CS nanocomposite was further evidenced by XRD analysis. Fig. 5 shows the XRD patterns of $AgNO_3$, TiO_2, chitosan, and Ag/TiO_2/CS nanocomposite. The characteristic peaks of the raw materials were generated at 35.5° ($AgNO_3$), 25.3° (TiO_2), and 19.7° (chitosan). These peaks suggest the highly crystalline nature of these three compounds, which is consistent with

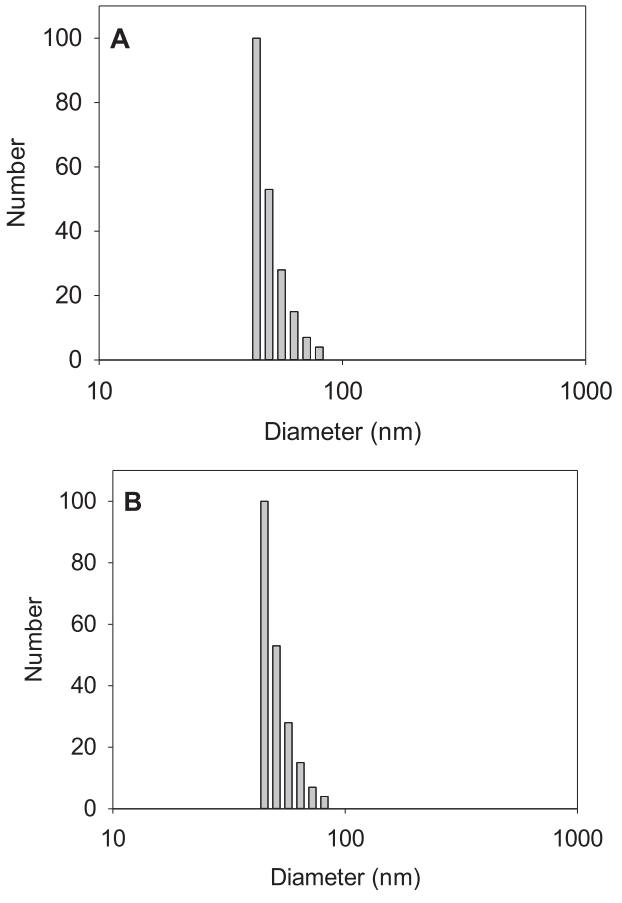

Fig. 2. Size distributions of Ag/TiO_2/CS nanocomposite (A: freshly prepared sample; B: sample stored for 60 days).

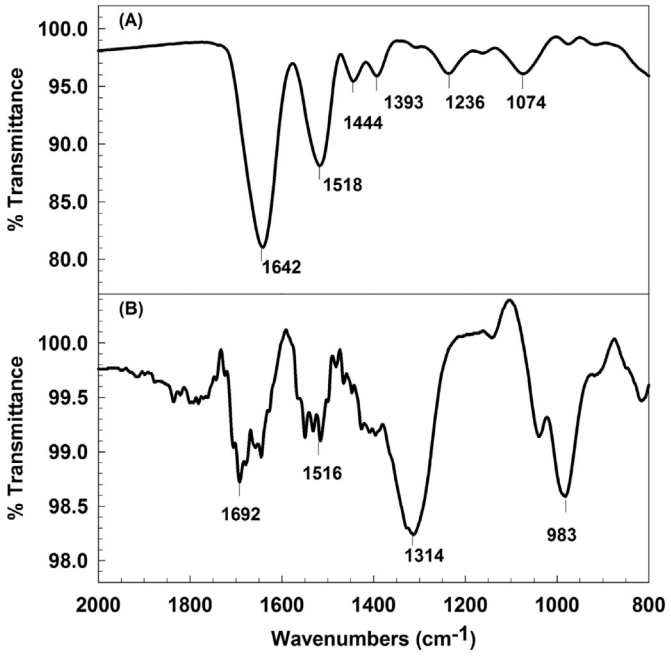

Fig. 3. The FTIR spectra of chitosan (A) and Ag/TiO_2/CS nanocomposite (B).

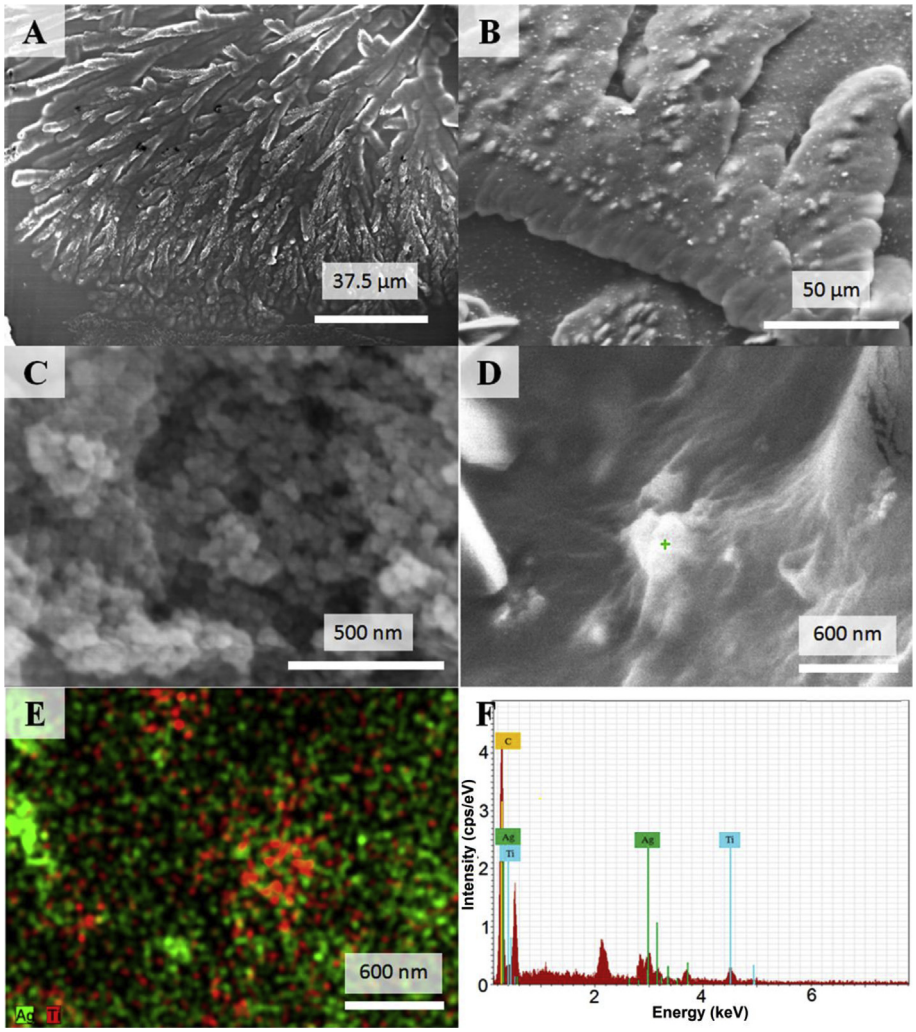

Fig. 4. SEM image of CS (A), Ag/TiO_2/CS nanocomposite (B, C, D), and EDS image (E) and plot (F) of Ag/TiO_2/CS nanocomposite showing elemental distribution of sample surface. The magnification factors were 4000 (A), 700 (B), 80,000 (C), 40,000 (D), and 40,000 (E).

existing literature (Au, Pham, Vu, & Park, 2012; Murugadoss & Chattopadhyay, 2008; Qi, Xu, Jiang, Hu, & Zou, 2004). These peaks are also observed in the XRD profile of nanocomposite, although with significantly lower intensities and minor shift to 38.4° (Ag), 21.6° (TiO_2), and 18.7° (chitosan). In addition, the peak corresponding to chitosan in the nanocomposite was wider than that in the profile for pure chitosan. These results indicated the successful incorporation of silver in the nanoscale CS matrix, which takes place mainly in the amorphous region of CS (Modrzejewska, Binias, Wojtasz-Pajak, Dorabialska, & Zarzycki, 2008).

3.5. Antibacterial assay

Ag nanoparticles, nano TiO_2, chitosan, Ag/CS and TiO_2/CS showed no inhibitory effect (0 mm diameter of inhibition) under the test conditions. However, $AgNO_3$ and Ag/TiO_2/CS nanocomposite showed a significant inhibitory effect with 10.5 ± 0.2 and 12.2 ± 0.7 mm diameter of inhibition, respectively. The solvation, absorption and diffusion of the samples are vital for the inhibition zone test (Kim et al., 2007). The relatively high solubility of $AgNO_3$ compared to other samples might explain its satisfactory performance. In addition, according to previous research, the inhibitory effect of chitosan depends on its molecular weight and degree of deacetylation (Jiang et al., 2013). Likewise, the inhibitory effect of nano-Ag and TiO_2 was related to their particle size, shape and state of aggregation (Jiang et al., 2013). These factors might account for the poor performance of the above-mentioned samples. On the contrary, the Ag/TiO_2/CS nanocomposite had a larger zone of inhibition than $AgNO_3$ indicating a more potent inhibitory effect than the other samples. This might be attributable to the better water solubility and stability against aggregation of adipic acid-modified chitosan nanoparticles. There are no existing reports regarding Ag/TiO_2/CS nanocomposite, to the best of our knowledge. We predicted that nanocomposite of Ag/TiO_2/CS would show better antibacterial performance based on the results of other test methods.

Table 1
Elemental analysis (EDS) of a nanocomposite particle shown in SEM image (Fig. 4E).

Element	Atomic count (%)	Error
C	88.94	5.9
Ti	5.32	0.5
Ag	5.74	0.9

3.6. Bactericidal efficacy in solution

As shown in Table 2, only Ag/TiO_2/CS nanocomposite showed antibacterial effect, reducing the *E. coli* concentration by 6 log to 3.2×10^3 CFU/mL after 24 h of incubation, while all other samples

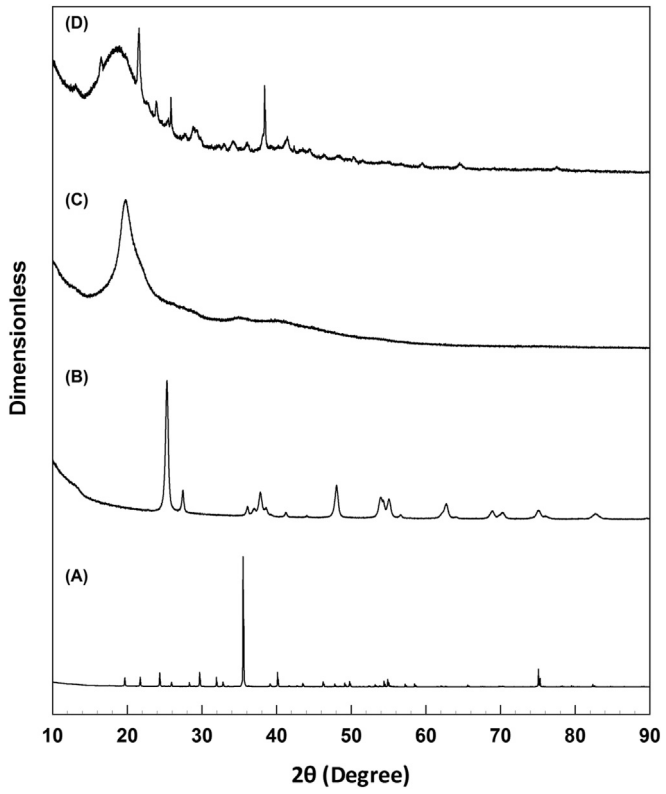

Fig. 5. XRD patterns of $AgNO_3$(A), TiO_2(B), chitosan(C)and Ag/TiO_2/CS nanocomposite(D).

as well as the TSB control (marked as CK) showed bacterial counts above 10^9 CFU/mL. These data indicate that the novel nanocomposite has superior bactericidal effect.

The minimum inhibitory concentration (MIC) of Ag/TiO_2/CS nanocomposite was then determined. The MIC of Ag/TiO_2/CS nanocomposite against *E. coli* was found to be 0.38 μg Ag/mL. Values of MIC obtained for Ag/TiO_2, $AgNO_3$, and nano-Ag are 1, 10, 4–6.75 μg Ag/mL, respectively, and chitosan has a MIC greater than 24 μg/mL (Jiang et al., 2013; Rodríguez-Argüelles, Sieiro, Cao, & Nasi, 2011; Zhang, Luo, & Wang, 2011). Clearly, the MIC of Ag/TiO_2/CS is much lower than that of $AgNO_3$ and nano-silver, indicating that the novel nanocomposite is effective in killing bacteria at lower concentrations.

The superior antimicrobial activity of the nanocomposite is also evidenced by the growth curve (Fig. 6), which shows that the Ag/TiO_2/CS nanocomposite (S3 and S4, representing the freshly prepared sample and the one that was stored for 60 days, respectively) exhibited stronger antibacterial ability against *E. coli* than controls, including CS (S1), $AgNO_3$ (S2), TiO_2 (S5), and nanosilver (S10). The fact that the curves for S3 and S4 do not show significant difference ($P < 0.05$) implies the desirable stability of the nanocomposite resulting from the high surface charge. The antibacterial ability of $AgNO_3$ (S2) was higher ($P < 0.05$) than that of nanosilver (S10) during the first 10 h. However, the difference became insignificant over the following 5 h. Thereafter, nanosilver exhibited higher activity than the $AgNO_3$ solution. In addition, the nanocomposite exhibited desirable antibacterial activities, possibly owing to its high dispersibility and the interaction with negatively charged biological membranes.

Table 2
Inhibition by different samples against *E. coli* in TSB Medium.[a]

Sample	Microorganism concentration (CFU/mL) bacterial level
Ag/TiO_2/CS[b]	3.2×10^3
Chitosan	4.0×10^9
Nano-Ag	3.9×10^9
$AgNO_3$	5.3×10^9
TiO_2	7.3×10^9
Ag/CS	5.2×10^9
TiO_2/CS	5.6×10^9
TSB[c]	6.6×10^9

[a] The concentration of compounds used is 100 μg/mL. The culture was incubated at 37 °C.
[b] CS means Chitosan.
[c] TSB was regarded as control.

3.7. The wettability of nanocomposite on cantaloupe rind

Ultimately, the affinity of the coating solution for the coating surface is very important. In this study, the contact angles of nanocomposite and water on cantaloupe rind were measured to determine the wettability. As shown in Fig. 7, the contact angle of nanocomposite on cantaloupe rind was 88.4 ± 0.16°, which was slightly greater than that of water (86.8 ± 6.3°), and remained stable for the duration of measurement. It should be noted that the change in the wettability of the nanocomposite is considerably smaller than that of water. This result indicates that cantaloupe rind is hydrophilic, and that the nanocomposite solution could attach to the rind more tightly than water.

4. Conclusions

A novel nanocomposite of Ag/TiO_2/CS was successfully prepared by photochemical reduction method and characterized. The nanocomposite exhibited small particle size and highly positive surface charges, which ensured its storage stability. Chitosan adipate not only acted as a reducing agent for the metal ions but also stabilized the product possibly through the Ag—N coordination bonds. The nanocomposite inhibited the growth of microorganisms markedly and more effectively than chitosan, $AgNO_3$, and nano-Ag particles. The MIC value of Ag/TiO_2/CS was 0.38 μg Ag/mL, which

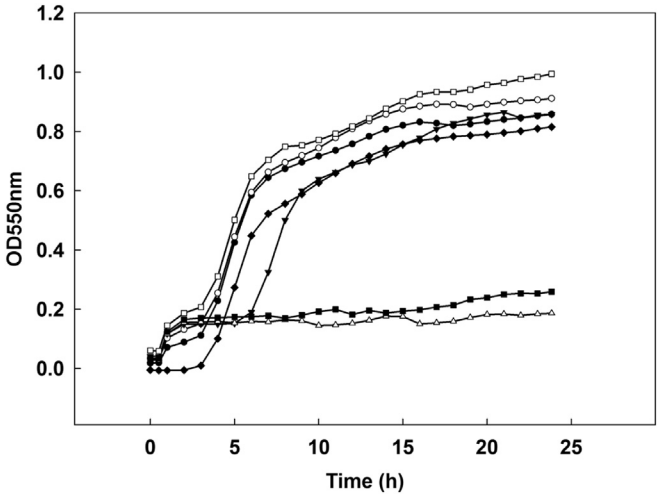

Fig. 6. The growth curve of *E. coli* O157:H7 in nanocomposite solution. Optical density (OD) of the *E. coli* culture containing different antimicrobial compounds was measured at 550 nm. The culture was incubated at 37 °C. The control is TSB broth at pH 7.0. Compounds tested are control (●), chitosan (S1, ○), $AgNO_3$ (S2, ▼), Fresh Ag/TiO_2/CS nanocomposite (S3, Δ), Ag/TiO_2/CS after 60 day storage (S4, ■), TiO_2 (S5, □), and nanosilver (S10, ◆). The concentration of all compounds was 100 μg/mL.

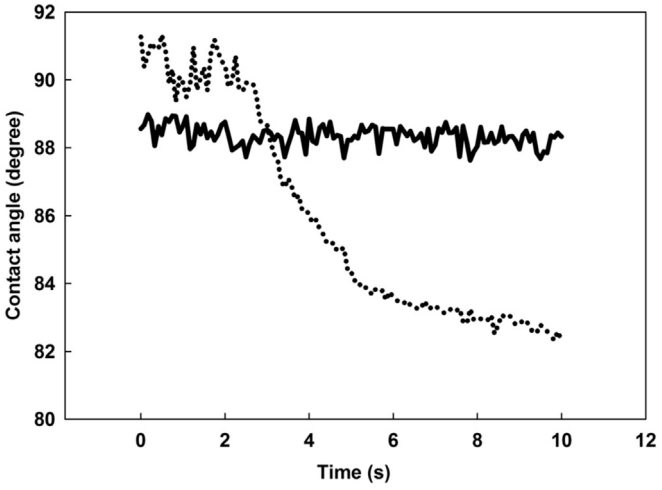

Fig. 7. The surface wettability of cantaloupe rind to nanocomposite solution (solid line) and water (dashed lines).

was significantly lower than those of chitosan, $AgNO_3$, or nano-Ag particles. Moreover, once applied, the nanocomposite was able to evenly attach on the pericarps of cantaloupes and remained stable even in the presence of cracks, thus potentially preventing bacteria from entering the crevices that are distinctive of cantaloupe rind. The results of this study suggest that application of the product as a coating would be beneficial for maintaining the quality and extending the shelf life of cantaloupes or other fruits. Further investigation may focus on safety and toxicity of this coating, including whether nanoparticles could migrate from coating to fruit and pose a risk for human consumption.

Acknowledgments

This research is supported by the USDA-NIFA Specialty Crop Research Initiative Grant Award No. 2010-51181-21230, and by National Natural Science Foundation of China under Grant No.51263001(to Baofeng Lin). We are grateful for the technical support of the Maryland NanoCenter of the University of Maryland, and to Ms. Ellen Turner at USDA-ARS.

References

Au, H. T., Pham, L. N., Vu, T. H. T., & Park, J. S. (2012). Fabrication of an antibacterial non-woven mat of a poly (lactic acid)/chitosan blend by electrospinning. *Macromolecular Research, 20*(1), 51–58.

Banerjee, S., Gopal, J., Muraleedharan, P., Tyagi, A. K., & Raj, B. (2006). Physics and chemistry of photocatalytic titanium dioxide: visualization of bactericidal activity using atomic force microscopy. *Current Science, 90*(10), 1378–1383.

Belalia, R., Grelier, S., Benaissa, M., & Coma, V. (2008). New bioactive biomaterials based on quaternized chitosan. *Journal of Agricultural and Food Chemistry, 56*(5), 1582–1588.

Bouazza, S., Alonzo, V., & Hauchard, D. (2009). Synthesis and characterization of Ag nanoparticles-polyaniline composite powder material. *Synthetic Metals, 159*(15), 1612–1619.

Byeon, J. H., & Kim, Y.-W. (2012). A novel polyol method to synthesize colloidal silver nanoparticles by ultrasonic irradiation. *Ultrasonics Sonochemistry, 19*(1), 209–215.

Carlson, C., Hussain, S. M., Schrand, A. M., Braydich-Stolle, L. K., Hess, K. L., Jones, R. L., et al. (2008). Unique cellular interaction of silver nanoparticles: size-dependent generation of reactive oxygen species. *The Journal of Physical Chemistry B, 112*(43), 13608–13619.

Du, W.-L., Niu, S.-S., Xu, Y.-L., Xu, Z.-R., & Fan, C.-L. (2009). Antibacterial activity of chitosan tripolyphosphate nanoparticles loaded with various metal ions. *Carbohydrate Polymers, 75*(3), 385–389.

Egerton, T. A., & Tooley, I. R. (2004). Effect of changes in TiO_2 dispersion on its measured photocatalytic activity. *The Journal of Physical Chemistry B, 108*(16), 5066–5072.

Geisberger, G., Gyenge, E. B., Hinger, D., Käch, A., Maake, C., & Patzke, G. R. (2013). Chitosan-thioglycolic acid as a versatile antimicrobial agent. *Biomacromolecules, 14*(4), 1010–1017.

Guzmán, M. G., Dille, J., & Godet, S. (2009). Synthesis of silver nanoparticles by chemical reduction method and their antibacterial activity. *International Journal of Chemical and Biomolecular Engineering, 2*(3), 104–111.

Hadrup, N., & Lam, H. R. (2014). Oral toxicity of silver ions, silver nanoparticles and colloidal silver–a review. *Regulatory Toxicology and Pharmacology, 68*(1), 1–7.

Hettiarachchi, M. A., & Wickramarachchi, P. (2011). Synthesis of chitosan stabilized silver nanoparticles using gamma ray irradiation and characterization. *Journal of Science of the University of Kelaniya Sri Lanka, 6*, 65–75.

Holowachuk, S. A., Bal'a, M. F., & Buddington, R. K. (2003). A kinetic microplate method for quantifying the antibacterial properties of biological fluids. *Journal of Microbiological Methods, 55*(2), 441–446.

Hu, B., Wang, S.-B., Wang, K., Zhang, M., & Yu, S.-H. (2008). Microwave-assisted rapid facile "green" synthesis of uniform silver nanoparticles: self-assembly into multilayered films and their optical properties. *The Journal of Physical Chemistry C, 112*(30), 11169–11174.

Jiang, L., Wang, F., Han, F., Prinyawiwatkul, W., No, H. K., & Ge, B. (2013). Evaluation of diffusion and dilution methods to determine the antimicrobial activity of water-soluble chitosan derivatives. *Journal of Applied Microbiology, 114*(4), 956–963.

Kim, J. S., Kuk, E., Yu, K. N., Kim, J.-H., Park, S. J., Lee, H. J., et al. (2007). Antimicrobial effects of silver nanoparticles. *Nanomedicine: Nanotechnology, Biology and Medicine, 3*(1), 95–101.

Kochkodan, V., Tsarenko, S., Potapchenko, N., Kosinova, V., & Goncharuk, V. (2008). Adhesion of microorganisms to polymer membranes: a photobactericidal effect of surface treatment with TiO_2. *Desalination, 220*(1), 380–385.

Lin, B., Du, Y., Liang, X., Wang, X., Wang, X., & Yang, J. (2011). Effect of chitosan coating on respiratory behavior and quality of stored litchi under ambient temperature. *Journal of Food Engineering, 102*(1), 94–99.

Lin, B. F., Wang, W., Li, Y. M., Liang, X. Q., & Du, Y. M. (2012). Conversion of chitosan to facilitate preparation of chitosan carboxylic salt with moisture absorption-retention abilities. *Advanced Materials Research, 396*, 2193–2197.

Luo, Y., Zhang, B., Cheng, W.-H., & Wang, Q. (2011). Preparation, characterization and evaluation of selenite-loaded chitosan/TPP nanoparticles with or without zein coating. *Carbohydrate Polymers, 82*(3), 942–951.

Lu, X., Zhang, B., Wang, Y., Zhou, X., Weng, J., Qu, S., et al. (2011). Nano-Ag-loaded hydroxyapatite coatings on titanium surfaces by electrochemical deposition. *Journal of The Royal Society Interface, 8*(57), 529–539.

Ma, G., Yang, D., Zhou, Y., Xiao, M., Kennedy, J. F., & Nie, J. (2008). Preparation and characterization of water-soluble *N*-alkylated chitosan. *Carbohydrate Polymers, 74*(1), 121–126.

Modrzejewska, Z., Binias, D., Wojtasz-Pajak, A., Dorabialska, M., & Zarzycki, R. (2008). Crystalline structure of chitosan microgranules cross-linked with Cu_2^+ and Ag^+ ions. *Crystal Growth and Design, 8*(12), 4372–4377.

Murugadoss, A., & Chattopadhyay, A. (2008). A 'green' chitosan-silver nanoparticle composite as a heterogeneous as well as micro-heterogeneous catalyst. *Nanotechnology, 19*(1), 015603.

Nadagouda, M. N., Speth, T. F., & Varma, R. S. (2011). Microwave-assisted green synthesis of silver nanostructures. *Accounts of Chemical Research, 44*(7), 469–478.

Ollar, R. A., Brown, S., Dale, J. W., Felder, M. S., Brown, I. N., Edwards, F. F., et al. (1991). A modified broth dilution assay for antibiotic sensitivity testing of *Mycobacterium avium-intracellulare* using paraffin slide cultures. *Tubercle, 72*(3), 198–205.

Onishi, H., & Machida, Y. (1999). Biodegradation and distribution of water-soluble chitosan in mice. *Biomaterials, 20*(2), 175–182.

Park, E.-J., Bae, E., Yi, J., Kim, Y., Choi, K., Lee, S. H., et al. (2014). Repeated-dose toxicity and inflammatory responses in mice by oral administration of silver nanoparticles. *Environmental Toxicology and Pharmacology, 30*(2), 162–168.

Qi, L., Xu, Z., Jiang, X., Hu, C., & Zou, X. (2004). Preparation and antibacterial activity of chitosan nanoparticles. *Carbohydrate Research, 339*(16), 2693–2700.

Reidy, B., Haase, A., Luch, A., Dawson, K. A., & Lynch, I. (2013). Mechanisms of silver nanoparticle release, transformation and toxicity: a critical review of current knowledge and recommendations for future studies and applications. *Materials, 6*(6), 2295–2350.

Rodríguez-Argüelles, M. C., Sieiro, C., Cao, R., & Nasi, L. (2011). Chitosan and silver nanoparticles as pudding with raisins with antimicrobial properties. *Journal of Colloid and Interface Science, 364*(1), 80–84.

Spadaro, D., Barletta, E., Barreca, F., Curro, G., & Neri, F. (2010). Synthesis of PMA stabilized silver nanoparticles by chemical reduction process under a two-step UV irradiation. *Applied Surface Science, 256*(12), 3812–3816.

Tan, Y., Dai, X., Li, Y., & Zhu, D. (2003). Preparation of gold, platinum, palladium and silver nanoparticles by the reduction of their salts with a weak reductant-potassium bitartrate. *Journal of Materials Chemistry, 13*(5), 1069–1075.

Teng, Z., Luo, Y., & Wang, Q. (2012). Nanoparticles synthesized from soy protein: preparation, characterization, and application for nutraceutical encapsulation. *Journal of Agricultural and Food Chemistry, 60*(10), 2712–2720.

Tong, T., Binh, C. T. T., Kelly, J. J., Gaillard, J.-F., & Gray, K. A. (2013). Cytotoxicity of commercial nano-TiO_2 to *Escherichia coli* assessed by high-throughput screening: effects of environmental factors. *Water Research, 47*(7), 2352–2362.

Vásconez, M. B., Flores, S. K., Campos, C. A., Alvarado, J., & Gerschenson, L. N. (2009). Antimicrobial activity and physical properties of chitosan-tapioca starch based edible films and coatings. *Food Research International, 42*(7), 762–769.

Wei, D., Sun, W., Qian, W., Ye, Y., & Ma, X. (2009). The synthesis of chitosan-based silver nanoparticles and their antibacterial activity. *Carbohydrate Research, 344*(17), 2375–2382.

Yuan, W., Ji, J., Fu, J., & Shen, J. (2008). A facile method to construct hybrid multi-layered films as a strong and multifunctional antibacterial coating. *Journal of Biomedical Materials Research Part B: Applied Biomaterials, 85*(2), 556–563.

Zhang, B., Luo, Y., & Wang, Q. (2010). Development of silver-zein composites as a promising antimicrobial agent. *Biomacromolecules, 11*(9), 2366–2375.

Zhang, B., Luo, Y., & Wang, Q. (2011). Development of silver/α-lactalbumin nano-composites: a new approach to reduce silver toxicity. *International Journal of Antimicrobial Agents, 38*(6), 502–509.